Modeling of the depressurisation induced by a pipe rupture in the primary circuit of a nuclear plant

Marie-France Robbe* — Serguei Potapov**

* CEA Saclay, SEMT-DYN
F-91191 Gif sur Yvette cedex
mfrobbe@cea.fr or marie-france.robbe@cea.fr

** EDF, SEP/AMV
1 av. du Général de Gaulle
F-92140 Clamart
serguei.potapov@edf.fr

ABSTRACT. The safety analysis of Pressurised Water Reactors is based on the assessment of the consequences of a hypothetical Loss Of Coolant Accident. The accident supposes that a break occurs on a pipe of the primary circuit. A depressurisation wave propagates from the break through the entire primary circuit, then the circuit empties progressively in diphasic regime. The geometry of the primary circuit is simplified and represented with a pipe-model to be able to simulate the accident in the entire circuit. After a presentation of the geometry and the numerical model, the hydraulic consequences of the LOCA are analysed.

RÉSUMÉ. L'analyse de sûreté des Réacteurs à Eau Pressurisée est basée sur l'évaluation des conséquences d'un hypothétique Accident par Perte de Réfrigérant Primaire. L'accident suppose qu'une brèche se produit sur un tuyau du circuit primaire. Une onde de dépressurisation se propage dans l'ensemble du circuit primaire à partir de la brèche, puis le circuit se vide progressivement en régime diphasique. La géométrie du circuit primaire a été simplifiée et représentée par un modèle-tuyau afin de pouvoir simuler l'accident sur l'ensemble du circuit. Après une présentation de la géométrie et du modèle numérique, les conséquences de l'APRP sont analysées.

KEYWORDS: fast dynamics, hydraulic, numerical simulation, nuclear reactor.

MOTS-CLÉS : dynamique rapide, hydraulique, simulation numérique, réacteur nucléaire.

1. Introduction

The safety studies of the nuclear reactors (Libmann, 1996) are based on the analysis of the consequences of several hypothetical accidents. In the case of the Pressurised Water Reactors (PWR), one of the accidents taken into consideration is a Loss Of Coolant Accident (LOCA). This accident consists in the rupture of a pipe of the primary circuit. This circuit cools the core of the reactor and is essential for the reactor safety.

The rupture induces a blowdown at the break, which causes the propagation of an acoustic wave through the entire primary circuit, and an emptying of the circuit, first with a monophasic regime and later with a diphasic one. The local pressure gaps due to the propagation of the depressurisation wave may induce whippings of pipes, recoils of components or displacements of the internal structures.

During the 70s, the whipping of pipes (Cauquelin *et al.,* 1979) and their split (Dupuy *et al.,* 1983), the impact of pipes on bumpers (Caumette *et al.,* 1981), and the recoil force on the vessel (Garcia *et al.,* 1981) were studied with the Aquitaine II test-facility and the codes Tedel, Trico and Titus (Garcia *et al.,* 1982).

The acoustic response was assessed by a mono-dimensional modal analysis (Gibert, 1988) (Lepareux, 1974a) with the monophasic fluid represented by an added mass. The transfer function of the circuit was computed with the Vibraphone code (Lepareux, 1975) and the circuit response with the Transit code. Both codes had been validated (Lepareux, 1974b) by the Wham blowdown experiment (Gruen, 1970).

During the 80s, by using an improved modal approach (Jeanpierre *et al.,* 1979, Guilbaud *et al.,* 1983a) taking into account the fluid-structure interaction, the effects of the LOCA acoustic phase on the reactor internal structures (*Guilbaud et al.,* 1983b, Guilbaud, 1987) were calculated with a set of three codes: Tedel for the pipes, Aquamode for the axisymmetrical vessel with the internal structures and the fluid, and Tristana for the connections.

Afterwards, the Castem-Plexus code dedicated to the Fast Dynamics Analysis was able to carry out hydrodynamic calculations involving coupled acoustic-hydraulic-mechanical phenomena. After the validation of the Castem-Plexus code for pipe circuits (Lepareux *et al.,* 1985a, Lepareux *et al.,* 1985b, Millard *et al.,* 1985) on experiments (Couilleaux *et al.,* 1984), first calculations were performed on a HDR reactor (Schwab *et al.,* 1989, Lepareux *et al.,* 1991, HDR Sicherheltsprogramm, 1980) in which water was initially at rest and described by a simplified diphasic constitutive law.

During the 90s, the water constitutive law was much improved and simulations were carried out to assess the LOCA hydrodynamic effects in the primary circuit of a 3-loop PWR (Robbe *et al.,* 2002a). These simulations enabled to understand the

depressurisation phenomenon from approximate initial conditions and with a simple break model.

Since then, the Castem-Plexus code has been merged with the Plexis-3C code to increase the capacities of both codes. The new Europlexus code has been improved to initialise precisely the LOCA simulation with the PWR operating conditions. Besides, as the blowdown process depends much on the break conditions, several break models have been developed in order to simulate the diphasic regime of water at the break.

The numerical models implemented in Europlexus to represent the rupture of a pipe are described. Then the paper presents a hydrodynamic simulation of flows in the primary circuit of a 4-loop PWR during a LOCA. The results concern the propagation of the depressurisation acoustic wave along the circuit, coupled with the transient fluid flows.

2. Numerical models of Europlexus

2.1. *General description of the code*

Europlexus is a general Fast Dynamics computer code developed by the CEA-Saclay (Chavant *et al.,* 1979, Hoffmann *et al.,* 1984, Robbe *et al.,* 1994) and JRC-Ispra (Bung *et al.,* 1989). Its main applications (Robbe *et al.,* 1999) are impacts, explosions (Robbe *et al.,* 2001a, Robbe *et al.,* 2002b, Robbe *et al.,* 2002c, Robbe *et al.,* 2002d, Robbe *et al.,* 2002e), pipe transients, hydrodynamics (Struder *et al.,* 1997) and robots (Lepareux *et al.,* 1994a).

Europlexus is based on the Finite Element Method. The time resolution is explicit and realised with a Newmark algorithm. The code is devoted to the mechanical analysis of accidental situations in one, two or three dimensions, involving structures or fluids with different possibilities of coupling. The formulation can be either Lagrangian, Eulerian or A.L.E. (Arbitrary Lagrange Euler).

Europlexus can take into account various non-linearities related to materials or geometry. It computes successively, at each time step, the mass conservation, the total energy conservation, the material constitutive law and finally the momentum conservation.

The mass and total energy conservation laws are obtained by computing the flows between contiguous elements. The code solves the weak formulation of the momentum equation.

Mass conservation

$$M^{(n+1)} = M^{(n)} + \Delta M^{(n \rightarrow n+1)}$$

$$\text{with } \Delta M^{(n \to n+1)} = \int_{t^{(n)}}^{t^{(n+1)}} \oint_A \rho \, \vec{n} \cdot \vec{v} \, dA \, dt + \int_{t^{(n)}}^{t^{(n+1)}} \int_V M_{ext} \, dV \, dt$$

Total energy conservation

$$E^{(n+1)} = E^{(n)} + \Delta E^{(n \to n+1)}$$

$$\text{with } \Delta E^{(n \to n+1)} = \int_{t^{(n)}}^{t^{(n+1)}} \oint_A \rho \left(H + \frac{1}{2} \vec{v} \cdot \vec{v} \right) \vec{n} \cdot \vec{v} \, dA \, dt + \int_{t^{(n)}}^{t^{(n+1)}} \int_V E_{ext} \, dV \, dt$$

Weak formulation of the momentum conservation

$$\int_{t^{(n)}}^{t^{(n+1)}} \int_V \vec{U}^* \cdot \rho \frac{\partial \vec{v}}{\partial t} dV dt + \int_{t^{(n)}}^{t^{(n+1)}} \int_V \vec{U}^* \cdot \left(\rho \vec{v} \cdot \overline{\overline{\dot{\varepsilon}}} \right) dV dt - \int_{t^{(n)}}^{t^{(n+1)}} \oint_A \vec{n} \cdot \left(\vec{U}^* \cdot \overline{\overline{\sigma}} \right) dA dt + \int_{t^{(n)}}^{t^{(n+1)}} \int_V \overline{\overline{\varepsilon}}^* : \overline{\overline{\sigma}} dV dt = \int_{t^{(n)}}^{t^{(n+1)}} \int_V \vec{F}_{ext} dV dt$$

$M^{(n+1)} \, \vec{\gamma}^{(n+1)}$ transport force boundary conditions internal forces external forces

with

A	surface	$\vec{U}^*$	arbitrary displacement
E	total energy	V	volume
E_{ext}	external energy source	$\overline{\overline{\varepsilon}}^*$	strain (spatial derivative of $\vec{U}^*$)
H	total enthalpy	$\overline{\overline{\dot{\varepsilon}}}$	strain speed (spatial derivative of $\vec{v}$)
M	mass	$\vec{v}$	velocity
M_{ext}	external mass source	ρ	density
$\vec{n}$	normal vector	$\overline{\overline{\sigma}}$	stress
t	time		

2.2. *The constitutive laws*

2.2.1. *Water*

In a Pressurised Water Reactor, the primary circuit is filled with pressurised water. In the case of a Loss Of Coolant Accident, water flows out of the primary circuit and vaporises in and out the circuit.

In Europlexus, water and steam are described by a classical single water constitutive law including vaporisation but supposing an homogeneous mixture at thermodynamic equilibrium (Papon *et al.,* 1990, Lepareux, 1994b, Robbe *et al.,* 1996). The two phases are assumed to be at the same pressure and temperature and

there is no phase sliding. This constitutive law is also used for the computation of steam explosion accidents.

If P is pressure and T the temperature, the projection in the (T, P)-plane of the state equation of water shows the different phases of the material and the curves of fusion, vaporisation and sublimation (Figure 1). The diagram presents two particular points. The triple point T (0.01°C; 62 Pa) corresponds to the coexistence of three states: solid, liquid and steam. Beyond the critical point C (374°C, 22.1 MPa), it is impossible to distinguish liquid from steam; water is a monophasic fluid.
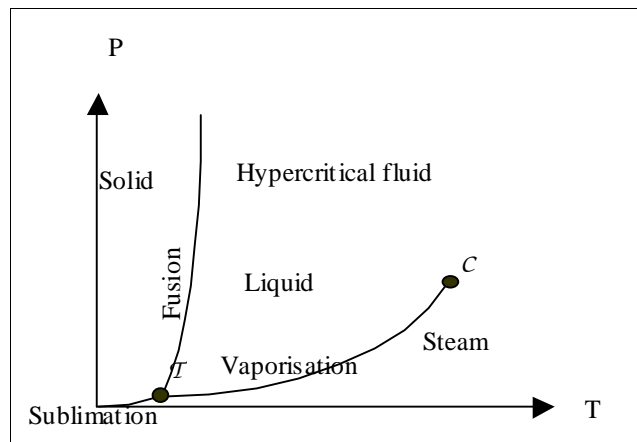
Figure 1. *Projection of the state equation in the (T, P)- plane*

Monophasic states (liquid or vapour in the subcritical field, gas in the supercritical field)

$$
\left\{
\begin{aligned}
\Delta P &= \frac{\left(\dfrac{\partial \vartheta}{\partial T}\right)_P \Delta H - \left(\dfrac{\partial H}{\partial T}\right)_P \Delta \vartheta}{\left(\dfrac{\partial \vartheta}{\partial T}\right)_P \left(\dfrac{\partial H}{\partial P}\right)_T - \left(\dfrac{\partial \vartheta}{\partial P}\right)_T \left(\dfrac{\partial H}{\partial T}\right)_P} \\[2em]
\Delta T &= \frac{\left(\dfrac{\partial H}{\partial P}\right)_T \Delta \vartheta - \left(\dfrac{\partial \vartheta}{\partial P}\right)_T \Delta H}{\left(\dfrac{\partial \vartheta}{\partial T}\right)_P \left(\dfrac{\partial H}{\partial P}\right)_T - \left(\dfrac{\partial \vartheta}{\partial P}\right)_T \left(\dfrac{\partial H}{\partial T}\right)_P}
\end{aligned}
\right.
$$

Diphasic states (liquid and vapour in the subcritical field)

$$
\begin{cases}
\Delta P = \dfrac{(\vartheta_v - \vartheta_l)\Delta H - (H_v - H_l)\Delta\vartheta}{(\vartheta_v - \vartheta_l)\left(\dfrac{\partial\vartheta}{\partial P}\right)_{sat} - (H_v - H_l)\left(\dfrac{\partial H}{\partial P}\right)_{sat}} \\[4ex]
\Delta\alpha = \dfrac{\left(\dfrac{\partial H}{\partial P}\right)_{sat}\Delta\vartheta - \left(\dfrac{\partial\vartheta}{\partial P}\right)_{sat}\Delta H}{(\vartheta_v - \vartheta_l)\left(\dfrac{\partial\vartheta}{\partial P}\right)_{sat} - (H_v - H_l)\left(\dfrac{\partial H}{\partial P}\right)_{sat}}
\end{cases}
$$

with
$$
\left(\frac{\partial\vartheta}{\partial P}\right)_{sat} = \alpha\left(\frac{\partial\vartheta}{\partial P}\right)_v + (1-\alpha)\left(\frac{\partial\vartheta}{\partial P}\right)_l
$$
$$
\left(\frac{\partial H}{\partial P}\right)_{sat} = \alpha\left(\frac{\partial H}{\partial P}\right)_v + (1-\alpha)\left(\frac{\partial H}{\partial P}\right)_l
$$

$\vartheta = \dfrac{1}{\rho}$, α is the void fraction.

From the variation of pressure, temperature and void fraction, Europlexus computes all the other thermodynamic variables at each time step. Water tables (Haar *et al.*, 1984) are implemented in the code; they indicate the thermodynamic parameters versus the three previously cited variables at some points. The exact values are interpolated in the tables.

2.2.2. *Distributed pressure loss*

The flow of water in a circuit induces friction against the inner wall of the pipes or in the elbows. The main consequence of this friction is the appearing of a pressure loss distributed along the pipe length that reduces the fluid velocity. The pressure loss is computed from the velocity and the density.

$$
\Delta P = -\frac{k\,\rho\,v^2}{2\,L}
$$

where L is the length of the pipe and k the pressure loss coefficient depending of the several geometric and hydraulic parameters (Idel'Cik, 1986).

A distributed pressure loss is modeled in Europlexus by a constitutive law. In that case, the element is described by two constitutive laws: the water constitutive law and the distributed pressure loss law.

2.3. *The pipe model*

A 1D mesh is composed of tube elements, aligned to form the branches of a pipe circuit. The branches are connected by junction elements. The boundary conditions and the hydraulic peculiarities of the circuit are represented by specific elements.

2.3.1. *The tube element*

The tube element (Galon *et al.,* 2001) possesses two nodes with one degree of freedom per node and a single point of integration, what leads to a uniform value of the variables associated to the element (pressure, density, etc.).

The local axis is oriented from the first node of the element towards the second node of the element, the orientation being defined by the numbering of the nodes in the mesh. The global axis is oriented from the element of lower number towards the element of higher number (Figure 2). When the global and local axes are oriented in opposite directions, the sign of the local variables changes to transfer them to the global axis, and vice versa.
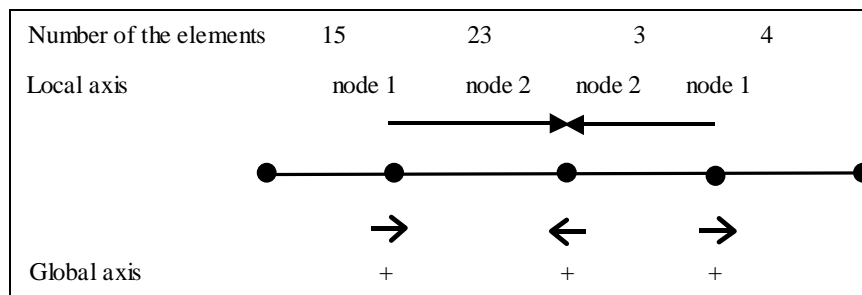
Figure 2. *Orientation of the tube elements*

Transport is computed considering the element that gives fluid. As the speed of particles is computed in the local axis of the element, flow is entering by the node 1 if the speed is positive and entering by the node 2 if the speed is negative.

The current element is noted *iel* and the neighbouring element is *jel*. At a given node *i*, the transports of mass and enthalpy are:

$$\Delta M_i = -\rho_{kel}^{(n)} \frac{\pi D_i^{\,2}}{4} \beta_i v_i^{(n+1/2)} \Delta t$$

$$\Delta H_i = -H_{kel}^{(n)} \frac{\pi D_i^{\,2}}{4} \beta_i v_i^{(n+1/2)} \Delta t$$

with D_i the diameter of the tube at the node i, $\beta_i = 1$ at the node 1 and $\beta_i = -1$ at the node 2. If $\beta_i v_i \geq 0$, the element giving fluid *kel* is *jel*; if $\beta_i v_i < 0$, *kel = iel.*

2.3.2. *The element of junction*

An element of junction (Galon *et al.,* 2001) enables to join several parts of the circuit. It is possible to connect up to 9 tubes, so the number of nodes of the element varies between 1 and 9 according to the number of tubes to connect. The element ensures the conservation of the flows entering and going out of the junction.

In a first time, the flows of mass and enthalpy entering in the element are considered. If *iel, jel* and *i* indicate the element of junction, the elements connected to the junction and giving fluid, the node of the junction in front of the connected element, respectively, the density and enthalpy are obtained by the following equations, for the flows entering in the junction:

$$\rho_{iel}^{(n+1)} = \frac{1}{2}\left(\rho_{iel}^{(n)} + \frac{\sum_i \rho_{jel}^{(n+1)} D_i^2 v_i^{(n+1/2)}}{\sum_i D_i^2 v_i^{(n+1/2)}} \right)$$

$$H_{iel}^{(n+1)} = I_{iel}^{(n+1)} + \frac{P_{iel}^{(n+1)}}{\rho_{iel}^{(n+1)}}$$

where *I* is the internal energy, *P* the average pressure and *M* the average mass of the element.

$$I_{iel}^{(n+1)} = \frac{\sum_i \rho_{jel}^{(n+1)} D_i^2 v_i^{(n+1/2)} \dfrac{I_{jel}^{(n+1)}}{M_{jel}^{(n+1)}}}{\sum_i \rho_{jel}^{(n+1)} D_i^2 v_i^{(n+1/2)}}$$

$$P_{iel}^{(n+1)} = \frac{1}{2}\left(P_{iel}^{(n)} + \frac{\sum_i P_{jel}^{(n+1)} D_i^2 v_i^{(n+1/2)}}{\sum_i D_i^2 v_i^{(n+1/2)}} \right)$$

$$M_{iel}^{(n+1)} = \frac{\rho_{iel}^{(n+1)}}{V_{iel}}$$

In a second time, the continuity of flows is ensured by the method of the Lagrangian multipliers that consists in fact to impose:

$$\sum_{i} \rho_{i,kel}^{(n+1)} A_i \, v_i^{(n+1/2)} = 0$$

where $\rho_{i,kel}^{(n+1)}$ is the density of the element giving flow connected to the node i and A_i is the cross-section of the pipe connected to the node i.

2.3.3. *Local pressure loss*

A local pressure loss is defined using an element of boundary condition. This kind of element possesses 1 node with 1 degree of freedom and 1 point of integration.

The pressure loss is computed from the speed and the density of the element upstream the boundary condition:

$$\Delta P = -k \, \rho_{kel}^{(n+1)} \, \frac{v^{(n+1/2)} \left| v^{(n+1/2)} \right|}{2}$$

where *kel* is the element giving flow and k the pressure loss coefficient defined versus the geometric and hydraulic conditions (Idel'Cik, 1986).

2.3.4. *Pump*

A pump (Bliard *et al.,* 1995) is described by an element of boundary condition. A pump is defined by a pressure increment whose characteristic shape is $\Delta P = f(Q_v)$. $\Delta P = P_{down-steam} - P_{up-stream}$ and Q_v is the volume flow rate defined by:

$$\left| Q_v^{(n+1)} \right| = \frac{\pi D^2}{4} \left| v^{(n+1/2)} \right|$$

The user can provide any function to define the characteristic shape.

In normal operation, the pump accelerates the fluid, thus the pressure increment has the same sign as the velocity. In accidental operation, the speed may reverse or accelerate beyond the domain described by the characteristics. In both cases, the pump is considered out of order and $\Delta P = 0$.

2.3.5. *Break*

A break is also defined by a boundary condition. Several break models are available in Europlexus (Lepareux, 1997). When opening the break, water vaporises, the flow rate accelerates and is managed by the pressure difference between the fluid within the pipe and the atmosphere. However, the flow rate cannot exceed a maximal value called the critical flow rate. For diphasic flows, Moody (Moody, 1965) defines the critical flow rate by:

$$q_c = \sqrt{\frac{2\left[(h_u - h_l)(s_v - s_l) - (s_u - s_l)(h_v - h_l)\right]}{\left[\left(\frac{s_u - s_l}{s_v - s_l}\right)\frac{1}{\rho_v} + \left(\frac{s_v - s_u}{s_v - s_l}\right)\frac{K}{\rho_l}\right]^2 \left[(s_u - s_l) + \left(\frac{s_v - s_u}{K^2}\right)\right]}}$$

where the variables q_c, h, s and $K = v_v/v_l$ are the critical mass flow rate, the massic enthalpy, the massic entropy and the phase sliding ; the subscripts u, l and v refer to the up-stream fluid, liquid and steam.

The Moody model supposes a mono-dimensional annular flow, steady-state operating conditions, a pressure equilibrium between both phases, an isentropic flow and the conservation of the total energy.

3. Numerical model

3.1. *Geometry*

The main primary circuit of a 4-loop PWR is composed of a reactor and four primary loops, symmetrically located (Figure 3). Each loop contains a steam generator, a pump and three pipes: a hot leg, a U leg and a cold leg (Figure 4). Structures are assumed to remain fixed and infinitely rigid during the blowdown. Consequently, the model simulates only the hydraulic behaviour of water during depressurisation (Robbe *et al.*, 2000).

The hydraulic circuit is represented with a pipe model respecting the 3D-component capacities and the average distances covered by water. These two criteria are necessary to describe correctly the flow rates and the propagation times of the acoustic waves through the circuit.

For the components, the pipe length is evaluated using the average way of water inside each component. Figures 5 to 7 show the pipe model defined for the steam generators, the pumps and the reactor, respectively. The mesh of the complete circuit is presented in Figure 8. The break is simulated by adding a very short pipe, horizontal and perpendicular to the circuit in order to simulate a lateral leakage.
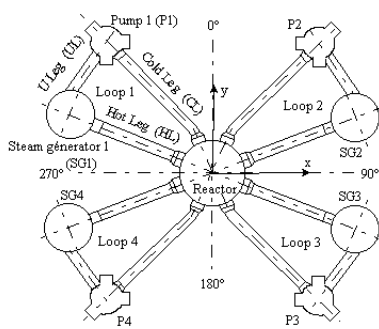
Figure 3. *The primary circuit (top view)*
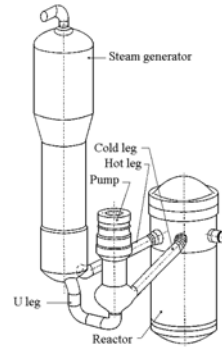
Figure 4. *A primary circuit loop*
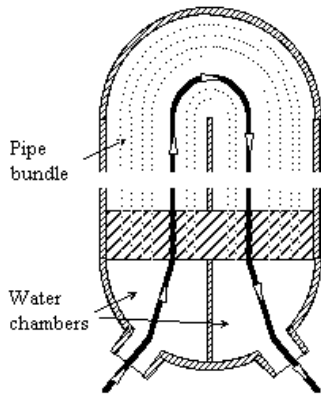
Figure 5. *The steam generator*
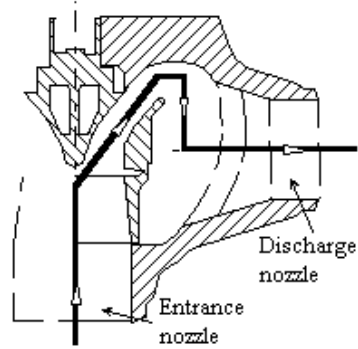
Figure 6. *The hydraulic part of the pum*
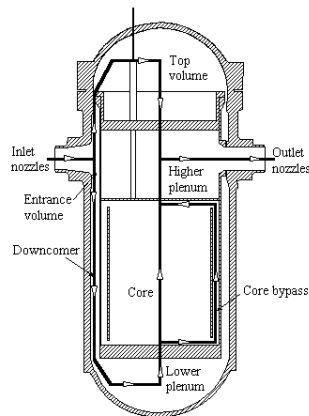
Figure 7. *The reactor*
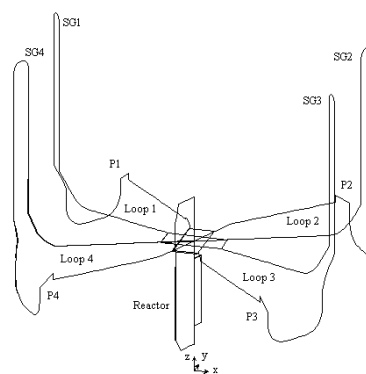
Figure 8. *Pipe model of the primary circuit of the reactor*

3.2. *Hydraulic model*

The core of a PWR is cooled by water. In order to guarantee that water remains liquid in operating conditions and during small classical transients, the primary circuit is pressurised. Hydraulic peculiarities, such as pump thrusts, pressure losses and the break, are applied by defining local boundary conditions or using specific constitutive laws. The characteristics of the pump (Figure 9) gives the increment of pressure versus the volume flow rate.
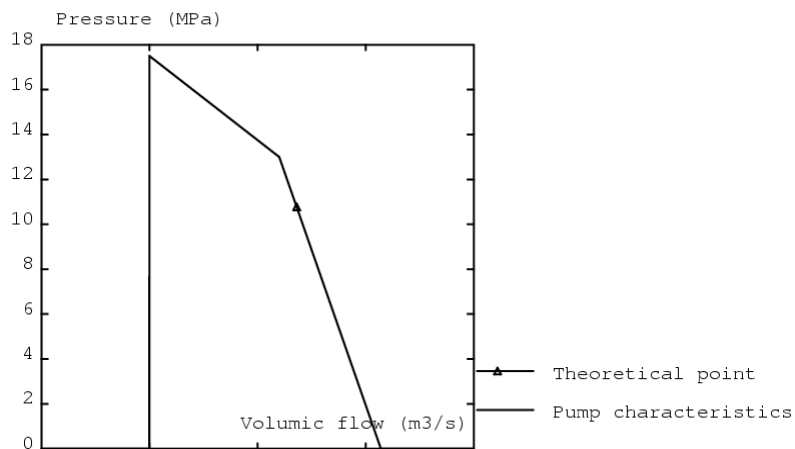
Figure 9. *Characteristics and working point of the pump*

Distributed pressure losses are applied to the legs, the tube bundles of the steam generators, the downcomer and the core (Figure 10). They are induced by friction along the inner surface of the pipes, direction changes of flow in the elbows, grid effects (distribution baffle of flow) and changes of cross-section in the steam generators, friction along the fuel assemblies in the core. The pressure loss coefficients are estimated for normal operation and kept for the accidental operation.

Local pressure drops are applied (Figure 11) at the level of the plates in the steam generators and the reactor, at the inlets and outlets of the reactor and the steam generators owing to the 1D-3D flow changes.

The restrictions of the cross-section at the inlet and outlet of the core bypass and the top volume are not geometrically represented, but the flow rate is imposed by means of a pressure drop equal to the one of the parallel circuit.
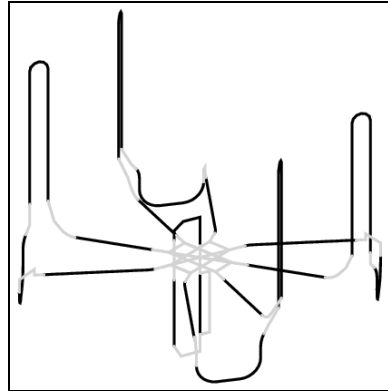
Figure 10. *Distributed pressure losses*   **Figure 11.** *Local pressure losses*
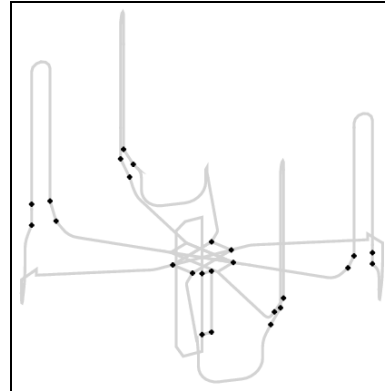
As the weldings on the structures constitute the weaker points of the circuit from the mechanical point of view, the most probable location for a pipe rupture is one of the weldings. Figure 12 presents the different locations envisaged for the break. Although the safety authorities require to study all the break locations, this presentation focuses on the break n°3, on the U leg of the first loop, just down-stream the steam generator. A conventional double-ended guillotine rupture is supposed to occur. The outside pressure is equal to 0.1 MPa and the tear lasts 1 ms.

Because the conditions at the break govern the dynamic transfers of mass in the entire primary circuit, it is essential to use a break model as realistic as possible. Among the models available in EUROPLEXUS the Moody's model was chosen because it includes a phase slide. Water, initially liquid, vaporises almost instantaneously and its speed is governed by the diphasic critical flow rate.
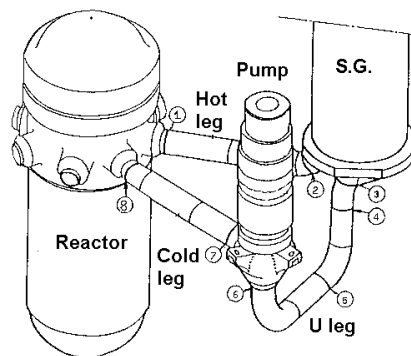
Figure 12. *The break location*

3.3. *Initial conditions*

The calculations are initialised at conditions as close as possible from the nominal rating of the reactor. The initial pressure is equal to 15.5 MPa. The temperature of the circuit is supposed to be constant and equal to 311°C. According to (Haar *et al.,* 1984), the water density and the sound velocity are equal to 702 kg/m^3 and 950 m/s, respectively.

The full flow rate is equal to 6.81 m^3/s per loop, what means 27.23 m^3/s at the inlet and outlet of the reactor. The ratio of flow crossing the top volume is 0.4% of the flow crossing the inlet of the reactor. Thus the main flow (in the downcomer, the lower plenum and the higher plenum) reaches 99.6% of the flow at the reactor inlet. The flow in the core is equal to 96.5% of the main flow and the remaining 3.5% are going through the core bypass.

3.4. *Initialisation at the nominal rating*

In order to initialise precisely the LOCA simulation with the operating conditions of the 4-loop PWR, the calculation is carried out first in normal operation for 1000 ms of physical time. Then the break is opened in 1 ms on the loop 1 and the computation goes on for 1000 ms more with LOCA conditions (Potapov *et al.,* 2000).

The purpose of computing the nominal rating is double. It allows an exact initialisation of the LOCA simulation and a checking of the model consistency. As the results issued from numerical simulations of LOCA in real reactors cannot be compared with theoretical or experimental results, the detection of a mistake in the numerical model is difficult. Thus a preliminary work of validation of the model is compulsory.

The validation is obtained by performing a computation of the normal operating conditions. The break extremity remains clogged. As computations are initialised approximately under operating conditions, the convergence of the results around the initial conditions is sufficient to prove that the model is correct.

Figures 13 and 14 illustrate the evolution of pressure and the volume flow rate versus time at different locations of the primary circuit. Both Figures show the results of the simulation under operating conditions and during the LOCA.

After 1 s of simulation, the computation of the operating conditions is stabilised around a numerical working point of the circuit. The computed average pressure is equal to 15.414 MPa with some slight variations due to the local and distributed pressure drops. The minimal and maximal pressures (respectively 15.082 and 15.747 MPa) are observed on both sides of the pumps. The volume flow rate is equal to about 7.1 m^3/s in the loops and to 28 m^3/s in the reactor.
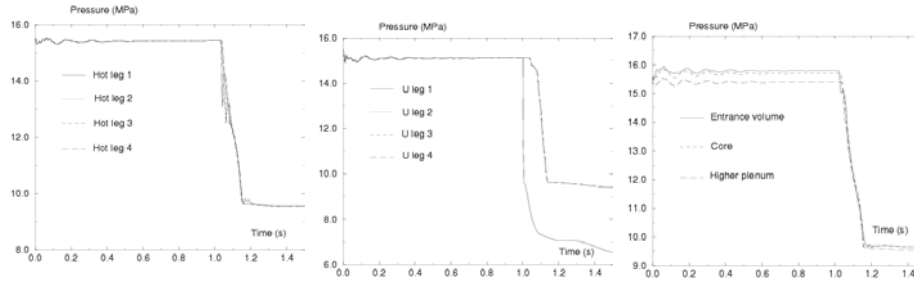
Figure 13. *Evolution of pressure throughout the simulation*
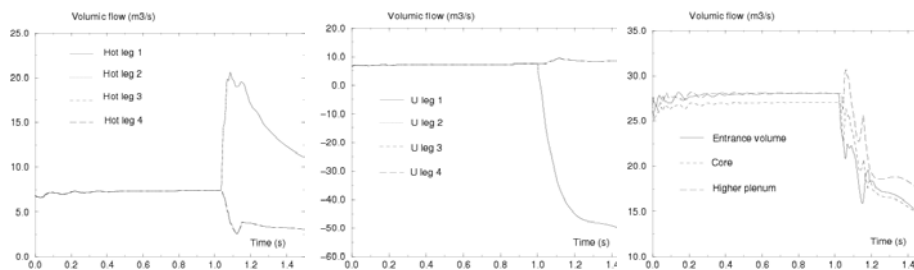
Figure 14. *Evolution of the volume flow rate throughout the simulation*

As the numerical working point computed under operating conditions is close to the theoretical working point, this preliminary step validates the numerical model. The simulation of the operating conditions providing results stable enough at 1 s, the simulation of the LOCA can start from that time.

4. Results of the simulation of the LOCA

Figure 15 shows the mass of water lost by the break. This curve is calculated by integrating the mass flow rate at the break. It presents the addition of the water lost by both pipe extremities. Globally, the mass of water increases linearly for the first 100 ms after the break opening. Then the mass increase becomes slightly curved. At 500 ms, 18 tons of water have been lost by the break.

Figures 16 to 20 present the evolution versus time of pressure, the volume flow rate, the void fraction, density and temperature, respectively (Robbe *et al.,* 2001b, Robbe *et al.,* 2001c, Robbe *et al.,* 2001d).
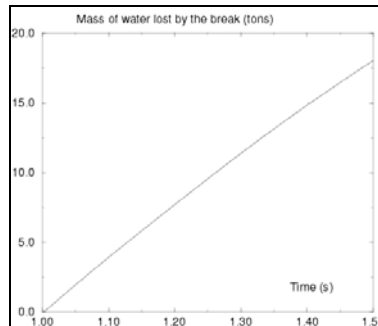
Figure 15. *Mass of water lost by the break*

Figure 16. *Pressure in the circuit*
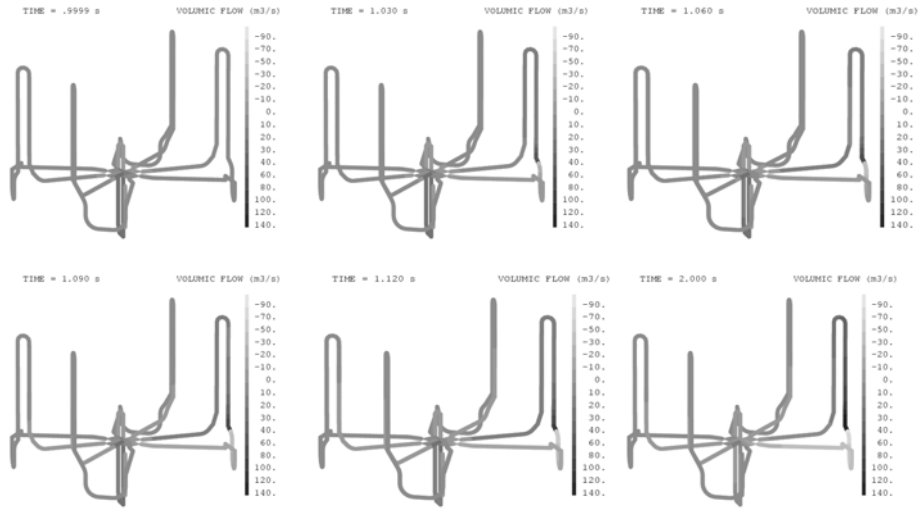
Figure 17. *Volume flow rate in the circuit*
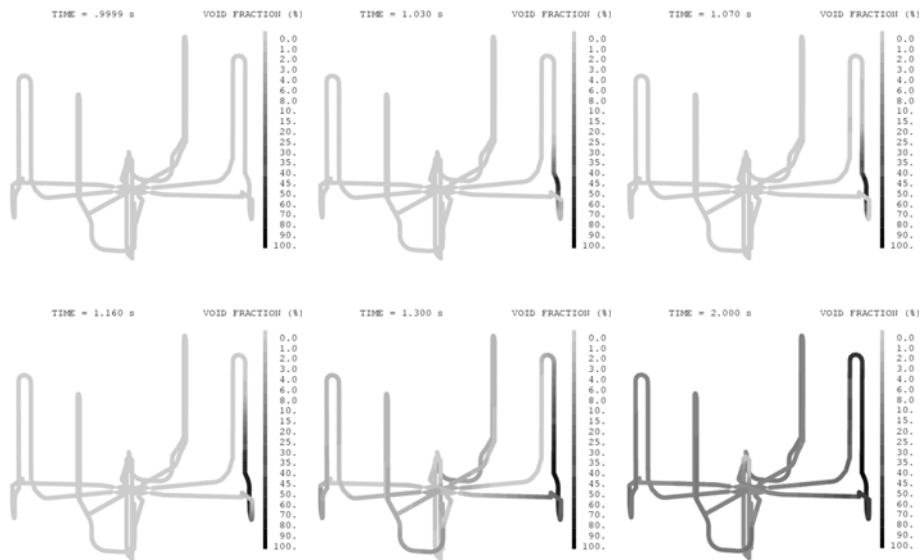
Figure 18. *Void fraction in the circuit*
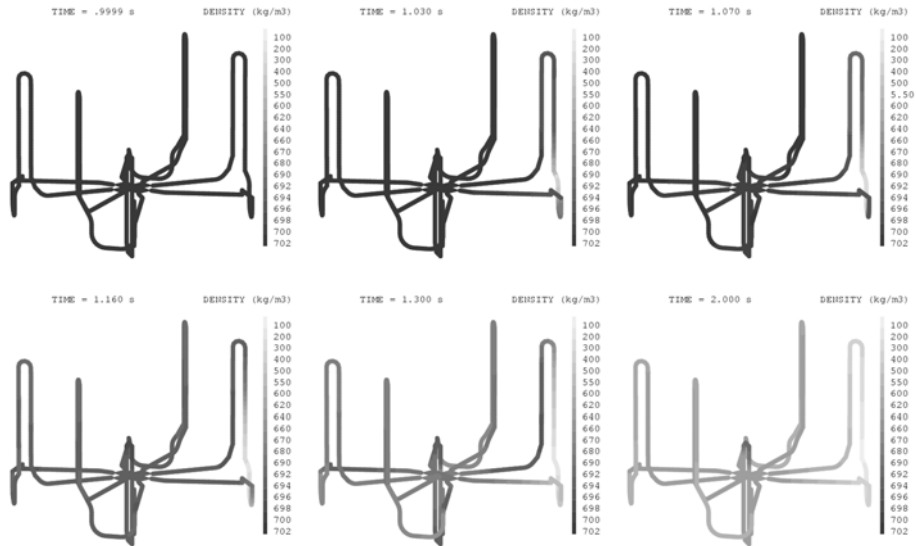
Figure 19. *Density in the circuit*
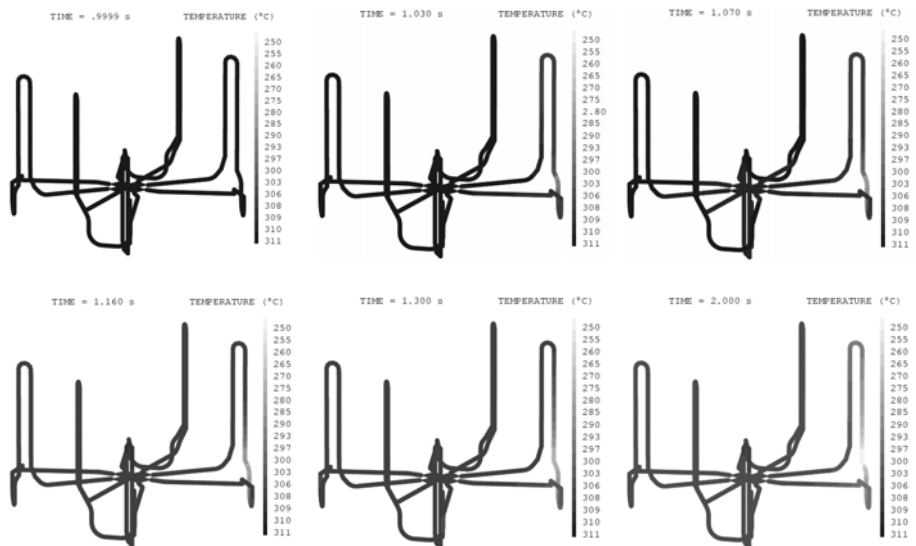
Figure 20. *Temperature in the circuit*

4.1. *First 10 ms of the LOCA*

During the first 2 ms after the rupture, a violent depressurisation happens at the break: pressure falls down to 6 MPa. Water starts vaporising because the saturation pressure is reached at the break: the void fraction reaches 55%. The rest of the circuit does not undergo yet the effects of the pipe rupture.

Between 2 and 8 ms, at the break, the effects of depressurisation become more marked. The void fraction reaches 70 % at 8 ms. The volume flow rate passes from 6.81 to 120 m^3/s because the high pressure difference between the loop end and the break accelerates water and because of the high steaming. Density falls from 702 kg/m^3 down to 300 kg/m^3 and temperature decreases from 311°C to 287°C. Between 2 and 10 ms, blowdown propagates in the break vicinity. Pressure falls down to about 9.5 MPa at 8 ms in the U leg 1 and at the outlet of the steam generator 1. In the U leg 1, the volume flow rate decreases before reversing. At the inlet of the steam generator 1, the volume flow rate increases up to 30 m^3/s. The break opening causes a flow rate decrease on the U leg side and a flow rate increase on the steam generator side. The void fraction starts increasing after 8 ms on both sides, as soon as the saturation pressure is reached.

4.2. *The LOCA between 10 and 50 ms*

From 10 to 20 ms, the blowdown wave 1 propagates from the break extremity in the U leg to the entrance volume of the reactor, causing a pressure decrease on the U leg side of the broken loop. In the U leg 1, the volume flow rate goes on decreasing, crosses zero at about 15 ms and then reverses.

Between 10 to 37 ms, the blowdown wave 2 propagates from the break extremity in the steam generator 1 to the higher plenum of the reactor. Pressure decreases on the steam generator side of the broken loop and the flow rate accelerates. Whereas the break opening causes an acceleration of the flow rate in the initial direction on the steam generator side, flow reverses and accelerates in the opposite direction on the U leg side.

After 20 ms, pressure decreases very slowly at the break and a bit faster in the break vicinity (in the U leg 1 and the steam generator 1). In the pump 1, water vaporises slightly between 20 and 40 ms when the saturation pressure is reached. The pump 1 stops working from 40 ms, when flow reverses in the pump. The pressure oscillations in the cold leg 1 are due to a partial reflection of the wave 1 against the junction between the loops and the reactor. Water condenses at 40 ms in the pump when the first pressure bump arrives.

In the reactor, the pressure fall is initiated by wave 1 between 20 and 37 ms on the inlet side: from the entrance volume to the bottom of the core and the bypass, and at the inlet of the top volume. Wave 2 initiates the fall between 37 and 59 ms on the

outlet side: from the higher plenum to the top of the core, at the top of the bypass and at the outlet of the top volume. Both pressure waves superimpose in the reactor from 37 ms. As in the broken loop, the passing of wave 1 causes a flow rate decrease whereas the passing of wave 2 causes a flow rate increase. Water remains liquid during this phase.

4.3. *The LOCA between 50 and 150 ms*

In the broken loop, the break and its vicinity are at saturation conditions, so pressure decreases slowly at the break, in the U leg 1 and at the outlet of the steam generator 1. In the cold leg 1 and the hot leg 1, the pressure continues decreasing to reach the saturation pressure at about 150 ms.

In the pump 1, several pressure bumps are caused by reflections of the blowdown wave against the junction with the reactor and by the emptying of the reactor containing liquid water. This slight pressure raise is sufficient to maintain water liquid until 100 ms.

At the inlet of steam generator 1, steaming is observed between 40 and 60 ms, and then a large pressure oscillation occurs between 60 and 145 ms owing to the passing of water coming from the reactor and the non-broken loops.

In the reactor, the pressure goes on decreasing until about 160 ms when the saturation pressure (9.5 MPa) is reached. Globally the flow rate decreases. However, large oscillations are recorded; they coincide with several passings and reflections of both blowdown waves. The flow does not change direction in the reactor, except at the inlet of the top volume where it reverses to supply with water the entrance volume.

In the non-broken loops, the wave 1 crosses the loops from the cold legs to the hot legs between 20 and 83 ms. The wave 2 passes in the opposite direction between 37 and 100 ms. Both blowdown waves induce a pressure decrease. The saturation pressure (9.5 MPa) is reached after about 150 ms. The flow rate does not change direction in the non-broken loops. However, the passing of wave 1 causes a flow rate increase while the passing of wave 2 causes a flow rate decrease.

The flow rate evolves in opposite way in the non-broken loops compared to the broken loop and the reactor. As the flow rate remains always positive and lower than 11 m^3/s in the non-broken loops, the pumps never stop working so that water is always pushed in the initial direction. Water remains liquid in the reactor and the non-broken loops.

The decrease of density and temperature is mainly caused by the pressure fall. In the broken loop, vaporisation induces an additional decrease. Globally, the density and the temperature in the circuit remain higher than 690 kg/m^3 and 308°C, except at

the break where they fall down to 300 kg/m^3 and 275°C after 150 ms and in the break vicinity where they decrease down to 400 kg/m^3 and 290°C, respectively.

In general, the different variables do not evolve much in the circuit until 50 ms: the broken loop is the only part of the circuit subject to major variations. Between 50 and 100 ms, the decrease of the different parameters propagates from the broken loop to the rest of the circuit (the flow rate is the single variable that increases in some parts of the circuit). After 100 ms, the entire circuit is subject to a global decrease. However, there is one exception: water vaporises only in the broken loop as long as 150 ms because pressure is higher than the saturation pressure anywhere else than in the broken loop.

4.4. *The LOCA between 150 and 500 ms*

After 150 ms, the pressure decreases very slowly. It remains equal to the saturation pressure in the whole circuit: approximately 9.5 MPa, apart from the break and in its vicinity where it is a bit lower (5 MPa at the break). At the inlet of the steam generator 1, pressure oscillates for the second time between 145 and 220 ms before stabilising; the amplitude of this oscillation is small, compared to the first one. This oscillation is due to the fact that water is still liquid in that part of the circuit, therefore the pressure in excess cannot be absorbed by a compression of steam.

At the break, the high increase of the void fraction (98% after 500 ms) induces a high increase of the volume flow rate (230 m^3/s at 500 ms) and a high decrease of density (140 kg/m^3) and temperature (260°C). In the break vicinity, the large steaming (70% in the U leg 1 and 65% at the outlet of the steam generator 1) has the same consequences, except that the volume flow rate increases in the opposite direction in the U leg 1.

In the cold part of the broken loop, the volume flow rate increases in the opposite direction and water vaporises. The density and the temperature go on decreasing; they evolve according to steaming. In the hot part of the broken loop, water is diphasic near the break but it remains liquid in the rest of the steam generator 1 and in the hot leg 1. This part of the circuit is the last one to vaporise. The decrease of the flow rate is caused by the progressive emptying of the circuit. The density and temperature present the same oscillations as those observed on the pressure curves as long as water does not vaporise; then the density and temperature decrease.

In the reactor, the volume flow rate globally decreases after 150 ms. However, there are some small oscillations while water remains liquid. In the bypass and the top volume, the flow rate is very low and the amplitude of the oscillations is high, compared to the average flow rate. The single flow reversal observed in the reactor is located at the inlet of the top volume.

In half the reactor on the inlet side, water vaporises at about 160 ms because the pressure decreases down to the saturation pressure. But water condenses almost immediately in the lower plenum and at the bottom of the core and the bypass. Vaporisation really starts after 400 ms. The density and temperature present a small trough around 160 ms corresponding to the short phase of vaporisation. Then they remain constant as long as water remains liquid. After 400 ms, the density and temperature decrease due to the increase of the steam rate.

In half the reactor on the outlet side, water vaporises from 150 ms and the steam rate augments with a logarithmic shape. The density and temperature globally decrease and their evolution is governed by the one of the void fraction. The top volume behaves a bit differently from the rest of the reactor: it is the last zone where water vaporises and, as the flow rate is very low in the top volume, the density and temperature decrease less than in the rest of the reactor.

In the non-broken loops, except in the cold legs, water starts steaming from 150 ms, since the saturation pressure is reached. Steaming causes a decrease of the flow rate between the hot legs and the U legs. In the cold legs and the pumps, the volume flow rate increases between 150 and 200 ms and decreases later. The pumps never stop working in the non-broken loops.

Between 300 and 500 ms, the volume flow rate rises in the U legs and at the outlet of the steam generators to become closer to the flow rates in the pumps and the cold legs. Globally, the volume flow rates are increasing from the hot legs to the cold legs. As the hot legs are no longer fed with water, they empty progressively. If the evolution of pressure and the void fraction is relatively uniform in the non-broken loops, the evolution of the volume flow rate depends much on the location in the loop.

The density and temperature are mainly governed by the evolution of the void fraction from 150 ms. Temperature roughly decreases from 308 to 306-307°C between 150 and 500 ms. Density decreases regularly from 150 ms, except in the cold legs where it remains stable until 400 ms. Due to the pump thrust, density reduces from the hot legs to the pumps but is higher in the cold legs.

The mass of water lost by the break increases linearly for the first 100 ms after the break opening and then increases a little more slowly. After 500 ms, 18 tons of water have been lost by the break.

On a general way, three parameters govern the blowdown: pressure, void fraction and the volume flow rate. Other variables can be deduced from them.

During the first 150 ms, the pressure influence is predominant in the major part of the circuit, due to the absence of steam. Only the broken loop is governed simultaneously by both pressure and the void fraction because of the influence of the break condition. After 150 ms, the void fraction dominates the evolution of the other variables (density, temperature).

5. Conclusion

In the frame of the safety studies for Pressurized Water Reactors, the analysis of the consequences of a hypothetical rupture of a pipe of the primary circuit is required. The purpose of this study consists in understanding the effects of the depressurisation of the circuit during the first milliseconds following the pipe rupture.

Since the blowdown process depends much on the break conditions and the evolution of pressure in the core is linked to the one in the complete circuit, it is necessary to simulate the accident in the complete primary circuit. The Europlexus code has been chosen to carry out the simulation of the accident because it is especially devoted to the analysis of fast transients.

As 3D simulations of the whole circuit are difficult to carry out, the geometry has been simplified and described by a pipe-model. The pipe model respects the 3D component capacities and the average distances covered by water, so that the acoustic transients and the mass transfers of fluid are correctly described.

In order to validate the numerical model and to initialise the LOCA simulation with the reactor operating conditions, a preliminary hydrodynamic simulation of the flows in operating conditions is carried out for 1 s in the primary circuit of a 4-loop reactor. Then a guillotine rupture is applied to one of the U legs and the simulation continues for 1 s more.

Six variables are examined in order to understand the phenomenon and its influence on the components of the primary circuit: pressure, volume flow rate, void fraction, density, temperature and the mass of water lost by the break. The analysis shows that the blowdown can be characterized by only three variables: pressure, void fraction and volume flow rate. The other variables are governed by the previous ones. A previous analysis of a LOCA in a 3-loop PWR (Robbe *et al.,* 2002a) has showed that a study of the evolution of the sound speed and the mass flow rate is not necessary as those variables are fully managed by the evolutions of pressure, density and the volume flow rate.

In the major part of the circuit, the depressurisation governs the transient process during the first 150 ms. Then pressure decreases down to the saturation pressure and vaporisation dominates the flow behaviour. From 150 ms, flow can be globally described by classical diphasic thermalhydraulic laws.

This simple pipe-model is able to provide a global idea of the blowdown progress in a PWR primary circuit in case of a guillotine rupture. Its main advantage comes from the short calculation time necessary to obtain numerical results and consequently its easiness to carry out parametrical studies regarding the break location or the break size.

In the future, 3D simulations of the reactor and coupled fluid-structure simulations will be carried out to improve the understanding of the accident.

6. Bibliography

Bliard F., Lepareux M., Programme PLEXUS, Modélisation d'un composant de type pompe, CEA report DMT/95-269, 1995.

Bung H., Casadei F., Halleux J.P., Lepareux M., "PLEXIS-3C: A computer code for fast dynamic problems for structures and fluids", *Proceedings of the tenth International Conference on Structural Mechanics In Reactor Technology SMIRT 10*, Vol. B, Anaheim, USA, August 1989, pp. 85-90.

Caumette P., Chouard P., Martin A., "Study of pipe rupture dynamics: Aquitaine II program", *Proceedings of the sixth International Conference on Structural Mechanics In Reactor Technology SMIRT 6*, paper F 8/4, Paris, France, August 1981.

Cauquelin C., Caumette P., Garcia J.L., Sermet E., "Experimental studies of PWR primary piping under LOCA conditions", *Proceedings of the fifth International Conference on Structural Mechanics In Reactor Technology SMIRT 5*, paper F 6/1, Berlin, Germany, August 1979.

Chavant C., Hoffmann A., Verpeaux P., Dubois J., "Plexus: A general computer code for explicit lagrangian computation", *Proceedings of the fifth International Conference on Structural Mechanics In Reactor Technology SMIRT 5*, paper B 2/8, Berlin, Germany, August 1979.

Couilleaux J., Lazare-Chopard G., Fouettement de tuyauteries RIC des paliers de 900 MWE, CEA report DEMT/SMTS/LAMS/84-26, 1984.

Dupuy A.P., Martin A., Thomas J.P., Garcia J.L., Caumette P., Chouard P., "Mechanical effects of breaks on PWR primary pipings, Analytical interpretation of tests", *Proceedings of the seventh International Conference on Structural Mechanics In Reactor Technology SMIRT 7*, paper F 1/4, Chicago, USA, August 1983.

Galon P., Lepareux M., Documentation théorique, Modélisation des tuyauteries dans EUROPLEXUS, CEA report SEMT/DYN/RT/01-021, 2001.

Garcia J.L., Caumette P., Huet J.L., "Studies of pipe whip and impact", *Proceedings of the sixth International Conference on Structural Mechanics In Reactor Technology SMIRT 6*, paper F 8/6, Paris, France, August 1981.

Garcia J.L., Martin A., Chouard P., "A simplified methodology for calculations of pipe impacts: comparison with tests", *Proceedings of the ASME conference Pressure Vessel and Piping*, Vol. 2, Phoenix, USA, 1982.

Gibert R.J., *Vibrations des structures. Interactions avec les fluides. Sources d'excitation aléatoires*, Collection de la Direction des Etudes et Recherches d'Electricité De France, Eyrolles, Paris, France, 1988, pp. 268-281.

Gruen G.E., Wham prediction of semiscale test results, USA Atomic Energy Commission Idaho Operations office, Contract n° AT(10-1)-123, 1970.

Guilbaud D., Gantenbein F., Gibert R.J., "A substructure method to compute 3D fluid-structure interaction during blowdown", *Proceedings of the seventh International Conference on Structural Mechanics In Reactor Technology SMIRT 7*, paper F 8/4, Chicago, USA, August 1983.

Guilbaud D., Gibert R.J., "Calculation of a HDR blowdown test using a substructure method", *Proceedings of the seventh International Conference on Structural Mechanics In Reactor Technology SMIRT 7*, paper B 10/1, Chicago, USA, August 1983.

Guilbaud D., "Dynamic response of PWR vessel during a blowdown", *Proceedings of the ninth International Conference on Structural Mechanics In Reactor Technology SMIRT 9*, Vol. F, Lausanne, Switzerland, August 1987.

Haar L., Gallagher J.S., Kell G.S., *NBS/NRC steam tables*, National Standard Reference Data System, 1984.

HDR Sicherheltsprogramm, Untersuchlungen von RDB Einbauten bei Bruch einer Reaktorühlmitteleitung, Quick look report, Vol. 29/2, Technischer Fachbericht, 1980, pp. 16-80.

Hoffmann A., Lepareux M., Schwab B., Bung H., "Plexus: A general computer program for fast dynamic analysis", *Proceedings of the Conference on Structural Analysis and Design on Nuclear Power Plant*, Porto Alegre, Brazil, 1984.

Idel'Cik I.E., *Memento des pertes de charge, Coefficients de pertes de charge singulières et de pertes de charge par frottement*, Collection de la Direction des Etudes et Recherche d'Electricité De France, Eyrolles, Paris, France, 1986.

Jeanpierre F., Gibert R.J., Hoffmann A., Livolant M., "Description of a general method to compute the fluid-structure interaction", *Proceedings of the fifth International Conference on Structural Mechanics In Reactor Technology SMIRT 5*, paper B 4/1, Berlin, Germany, August 1979.

Lepareux M., 1974., Rupture de la tuyauterie primaire dans Priam, Etude de la propagation de la dépressurisation dans la cuve pendant les premières millisecondes par le programme Vibraphone, CEA report EMT/74-179.

Lepareux M., Dépressurisation brusque, Comparaison des résultats du calcul de propagation (programme Vibraphone) avec une expérience, CEA report EMT/74-260, 1974.

Lepareux M., Système CEASEMT, Programme Vibraphone, CEA report EMT/75-40, 1975.

Lepareux M., Schwab B., Bung H., "Plexus: A general computer program for the fast dynamic analysis, The case of pipe-circuits", *Proceedings of the eighth International Conference on Structural Mechanics In Reactor Technology SMIRT 8*, paper F1 2/1, Brussels, Belgium, August 1985.

Lepareux M., Schwab B., Hoffmann A., Jamet P., Bung H., "Un programme général pour l'analyse dynamique rapide - Cas des tuyauteries", *Proceedings of the Colloque Tendances Actuelles en Calcul des Structures*, Bastia, France, 1985.

Lepareux M., Combescure A., Makil H., "Hydromechanical analysis of a primary pipe (1D) coupled to a reactor vessel (3D) during a depressurization", *Proceedings of the eleventh International Conference on Structural Mechanics In Reactor Technology SMIRT 11*, paper F 5/4, Tokyo, Japan, August 1991.

Lepareux M., Michelin J.M., Thiault D., Plexus-R: une extension de Plexus à la robotique, CEA report DMT/94-138, 1994.

Lepareux M., Programme PLEXUS, Matériau eau, Modèle homogène équilibré, CEA report DMT/94-398, 1994.

Lepareux M., Programme PLEXUS: les modèles de débit critique, CEA report DMT/97-29, 1997.

Libmann J., *Eléments de sûreté nucléaire*, IPSN, Les éditions de la physique, France, 1996.

Millard A., Jamet P, Lieutenant J.L., Schwab B., Goetsch D., "Whip analysis of guide-pipes of instrumentation below PWR vessels", *Proceedings of the eighth International Conference on Structural Mechanics In Reactor Technology SMIRT 8*, paper F1 4/7, Brussels, Belgium, August 1985.

Moody F.J., "Maximum flow rate of a single component two-phase mixture", *Journal of heat transfer*, February 1965.

Papon P., Leblond J., *Thermodynamique des états de la matière*, Editeurs des Sciences et des Arts, Hermann, Paris, France, 1990.

Potapov S., Robbe M.F., Téphany F., "Hydrodynamic consequences of a LOCA in a 4-loop PWR", *Proceedings of the European Congress on Computational Methods in Applied Sciences and Engineering ECCOMAS*, CD-rom, Barcelona, Spain, September 2000.

Robbe M.F., Lepareux M., Bung H., PLEXUS, Notice théorique, CEA report DMT/94-490, 1994.

Robbe M.F., Lepareux M., Programme PLEXUS, Matériau eau, Modèle homogène non équilibré, CEA report DMT/96-142, 1996.

Robbe M.F., Galon P., Yuritzinn T., "Castem-Plexus: un logiciel de dynamique rapide pour évaluer l'intégrité des structures en cas d'accident", *Proceedings of the fourth Conference INSTRUC*, Courbevoie, France, November 1999.

Robbe M.F., Potapov S., "A pipe-model to assess the hydrodynamic effects of a blowdown in a 4-loop PWR", *Proceedings of the eighth International Conference On Nuclear Engineering ICONE 8*, paper 8186, CD-rom, Baltimore, USA, April 2000.

Robbe M.F., Vivien N., Valette M., Berglas E., "Use of thermalhydraulic and mechanical linked computations to estimate the mechanical consequences of a steam explosion", *Journal of Mechanical Engineering*, Vol. 52, 2001, pp. 65-90.

Robbe M.F., Potapov S., Téphany F., "Modeling of the hydraulic flows in a 4-loop PWR with a pipe-geometry", *Proceedings of the ninth International Cconference On Nuclear Engineering ICONE 9*, paper 9864, CD-rom, Nice, France, April 2001.

Robbe M.F., Potapov S., Téphany F., "Estimation of the hydrodynamic effects of a LOCA in a 4-loop PWR", *Proceedings of the ninth International Cconference On Nuclear Engineering ICONE 9*, paper 9682, CD-rom, Nice, France, April 2001.

Robbe M.F., Potapov S., Téphany F., "Simulation of the blowdown induced by a LOCA in a 4-loop PWR", *Proceedings of the 1st ANS/HPS student conference, CD-rom, Texas A&M University*, College Station, USA, March 2001.

Robbe M.F., Lepareux M., Trollat C., "Hydrodynamic loads on a PWR primary circuit due to a LOCA", *Nuclear Engineering and Design*, Vol. 211, No 2-3, 2002, pp. 189-228.

Robbe M.F., Lepareux M., "Evaluation of the mechanical consequences of a steam explosion in a nuclear reactor", *Bulgarian Journal of Theoretical and Applied Mechanics*, Vol. 32, No 1, 2002, pp. 48-84.

Robbe M.F., Lepareux M., Treille E., Cariou Y., "Numerical simulation of an explosion in a simple scale model of a nuclear reactor", *Journal of Computer Assisted Mechanics and Engineering Sciences*, Vol. 9, No 4, 2002, pp. 489-517.

Robbe M.F., Bliard F., "A porosity method to describe the influence of internal structures on a fluid flow in case of fast dynamics problems", *Nuclear Engineering and Design*, Vol. 215, 2002, p. 217-242.

Robbe M.F., Lepareux M., Cariou Y., "Numerical interpretation of the MARA 8 experiment simulating a Hypothetical Core Disruptive Accident", *Nuclear Engineering and Design*, in press, 2002.

Schwab B., Lepareux M., Combescure A., Makil H., "Hydromechanical analysis of a primary pipe (1D) coupled to a reactor vessel (3D) during a depressurization", *Proceedings of the tenth International Conference on Structural Mechanics In Reactor Technology SMIRT 10*, paper T 6/1, Anaheim, USA, August 1989.

Struder E., Galon P., "Hydrogen combustion loads Plexus calculations", *Nuclear Engineering and Design*, Vol. 174, 1997, pp. 119-134.